Biochemistry

Structural Insights into Microbial One-Carbon Metabolic Enzymes Ni−Fe−S-Dependent Carbon Monoxide Dehydrogenases and Acetyl-CoA Synthases

Alison Biester, Andrea N. Marcano-Delgado, and Catherine L. Drennan*

Read Online

ACCESS | Metrics & More | Article Recommendations

ABSTRACT: Ni−Fe−S-dependent carbon monoxide dehydrogenases (CODHs) are enzymes that interconvert CO and CO_2 by using their catalytic Ni−Fe−S C-cluster and their Fe−S B- and D-clusters for electron transfer. CODHs are important in the microbiota of animals such as humans, ruminants, and termites because they can facilitate the use of CO and CO_2 as carbon sources and serve to maintain redox homeostasis. The bifunctional carbon monoxide dehydrogenase/acetyl-CoA synthase (CODH/ACS) is responsible for acetate production via the Wood−Ljungdahl pathway, where acetyl-CoA is assembled from two CO_2-derived one-carbon units. A Ni−Fe−S A-cluster is key to this chemistry. Whereas acetogens use the A- and C-clusters of CODH/ACS to produce acetate from CO_2, methanogens use A- and C-clusters of an acetyl-CoA decarbonylase/synthase complex (ACDS) to break down acetate en route to CO_2 and methane production. Here we review some of the recent advances in understanding the structure and mechanism of CODHs, CODH/ACSs, and ACDSs, their unusual metallocofactors, and their unique metabolic roles in the human gut and elsewhere.

Carbon monoxide dehydrogenase
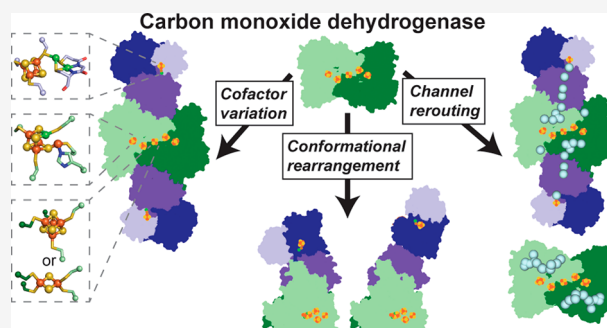
N i−Fe−S-dependent carbon monoxide dehydrogenases (CODHs) are thought to be early enzymes of life,[1] allowing microorganisms to live on the CO- and CO_2-rich atmospheres that were available at the time. The atmosphere has changed dramatically since these early times, but CODH-containing microorganisms are still prevalent. They exist where anoxic life is maintained, from bogs to cow rumens to the gut microbiota of organisms ranging from humans to termites.[2−4] CODHs are employed by microbes in a variety of metabolic roles, including CO oxidation, acetogenesis, and methanogenesis (Scheme 1 and Table 1).[5−7]

Monofunctional CODHs catalyze the reversible oxidation of CO to CO_2 in the biological equivalent of the water−gas shift reaction ($CO + H_2O \rightleftharpoons CO_2 + 2H^+ + 2e^-$).[5,6,8] They are used by a wide variety of microorganisms, including sulfate-reducing bacteria such as *Desulfovibrio vulgaris*, hydrogenogenic carboxydotrophs such as *Carboxydothermus hydrogenoformans*, and phototropic anaerobes such as *Rhodospirillum rubrum*. Collectively, CODH-catalyzed CO oxidation eliminates approximately 10^8 tons of CO from our environment annually (Scheme 1).[9] Although CO is toxic at high concentrations, CO plays useful roles in host−gut microbiome communication and is being explored as a therapeutic for inflammatory disorders.[10] To prevent the toxic effects of CO, it is hypothesized that CODH acts as CO sink in the gastrointestinal tract to maintain proper CO balance.[11]

Acetogens use CODHs as part of the Wood−Ljungdahl pathway of reductive acetogenesis (CO_2 to acetate).[6,8,12] This pathway generates acetyl-CoA from two molecules of CO_2 and eight reducing equivalents. It is responsible for the generation of approximately 10^9 tons of acetate per year, in which 10^7 tons come from acetogenic bacteria in the human gut (Scheme 1).[13−15] Acetogenic CODH is part of a bifunctional enzyme, carbon monoxide dehydrogenase/acetyl-CoA synthase (CODH/ACS). CODH reduces one CO_2 to CO (carbonyl branch), and ACS joins the resulting CO molecule with a methyl group that is provided by corrinoid iron−sulfur protein (CFeSP). This methyl group provided to ACS by CFeSP was generated by the reduction of the second molecule of CO_2 in the methyl branch of the pathway (Scheme 2).

In methanogenic archaea, CODH is also used in concert with ACS and CFeSP for carbon metabolism, though methanogens typically operate in the opposite direction relative to acetogens, such that methanogens break down acetyl-CoA to give methane and carbon dioxide (Scheme

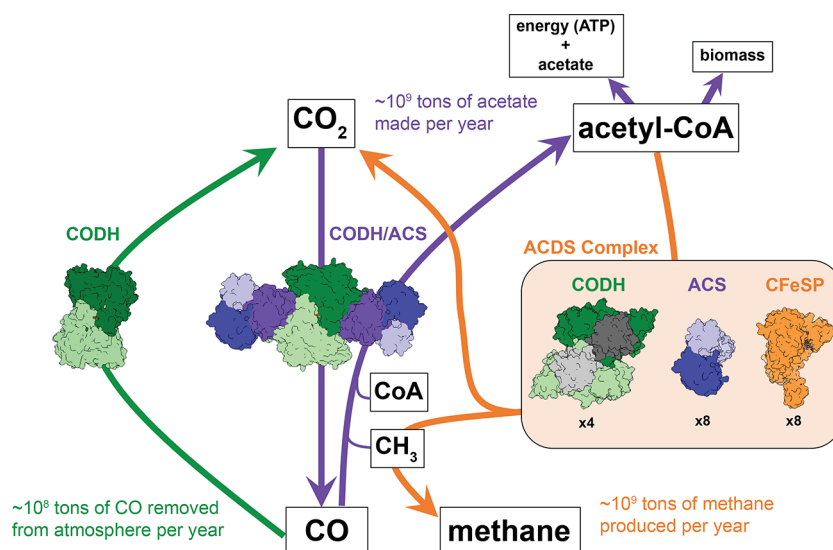**Scheme 1. CODH Enzymes Play Roles in CO Oxidation, Acetogenesis, and Methanogenesis[a]**


[a]CODH α_2 is colored light and dark green, and CODH ε_2 is colored light and dark gray. ACS domains 1−3 are colored violet, navy, and light blue, respectively. CFeSP is colored orange.

Table 1. CODH Variants

type of CODH	standard function[a]	oligomeric state	metallocofactors	published structures (PDB entry)
monofunctional CODH	CO oxidation	homodimeric	C-cluster for CO oxidation	*Rr*CODH (1JQK)
			B- and D-clusters for electron transfer	*Ch*CODH (1SU6, 1SU7, 1SU8, 1SUF, 2YIV, 3B51, 3B52, 3B53, 3I39, 4UDY, 5FLE, 6ELQ)
				*Dv*CODH (6B6V, 6B6W, 6B6X, 6B6Y, 6DC2, 6OND, 6ONS, 6VWY, 6VWZ, 6VX0, 6VX1, 7TSJ)
bifunctional CODH/ACS	CO$_2$ reduction and acetyl-CoA synthesis	heterotetramer $\alpha_2\beta_2$	C-cluster for CO$_2$ reduction	*Mt*CODH/ACS (1MJG, 6X5K, 2Z8Y, 3I04, 3I01, 1OAO)
			B- and D-clusters for electron transfer	*Ca*CODH/ACS (6YTT)
			A-cluster for acetyl-CoA synthesis	*Ch*ACS (1RU3)
ACDS	breakdown of acetyl-CoA and CO oxidation	$(\alpha_2\varepsilon_2)_4\beta_8(\gamma\delta)_8$	A-cluster for acetyl-CoA breakdown	*Mb*CODH (3CF4)
			C-cluster for CO oxidation	
			B- and D-clusters for electron transfer	
			E- and F-clusters of unknown function	
			corrinoid cofactor	

[a]The exact roles of these enzymes have not been established in many organisms. There could be different roles for monofunctional CODHs in different organisms.

Scheme 2. Wood−Ljungdahl Pathway of Acetogenesis[a]
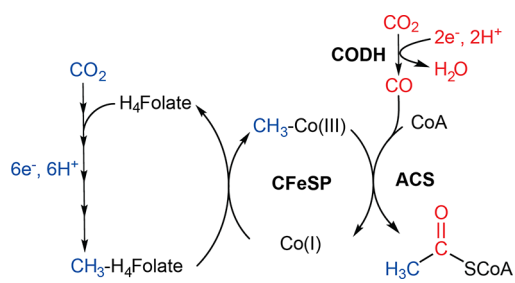
[a]The methyl branch is colored blue and the carbonyl branch is colored red.

1).[16,17] Unlike acetogenic CODH/ACS, which forms a transient complex with CFeSP, methanogenic CODH forms a stable complex with both ACS and CFeSP, called the acetyl-CoA decarbonylase/synthase complex (ACDS).[18,19] ACDS is an enormous 2.2 MDa $(\alpha_2\varepsilon_2)_4\beta_8(\gamma\delta)_8$ complex with four $\alpha_2\varepsilon_2$ CODH heterotetramers, eight β ACS monomers, and eight $\gamma\delta$ CFeSP heterodimers. A biological rationale for the large size of ACDS has not been established; the chemistry performed is no different from that of the acetogenic system. Methanogens are abundant in the human gut[3] and are believed to be responsible for the annual production of 10^9 tons of methane.[17]

Here we provide a brief review of some of the recent literature on stand-alone CODHs, CODH/ACSs, and ACDSs with a focus on structural data. By continued study of CODH structure, dynamics, and catalysis in various systems, we will
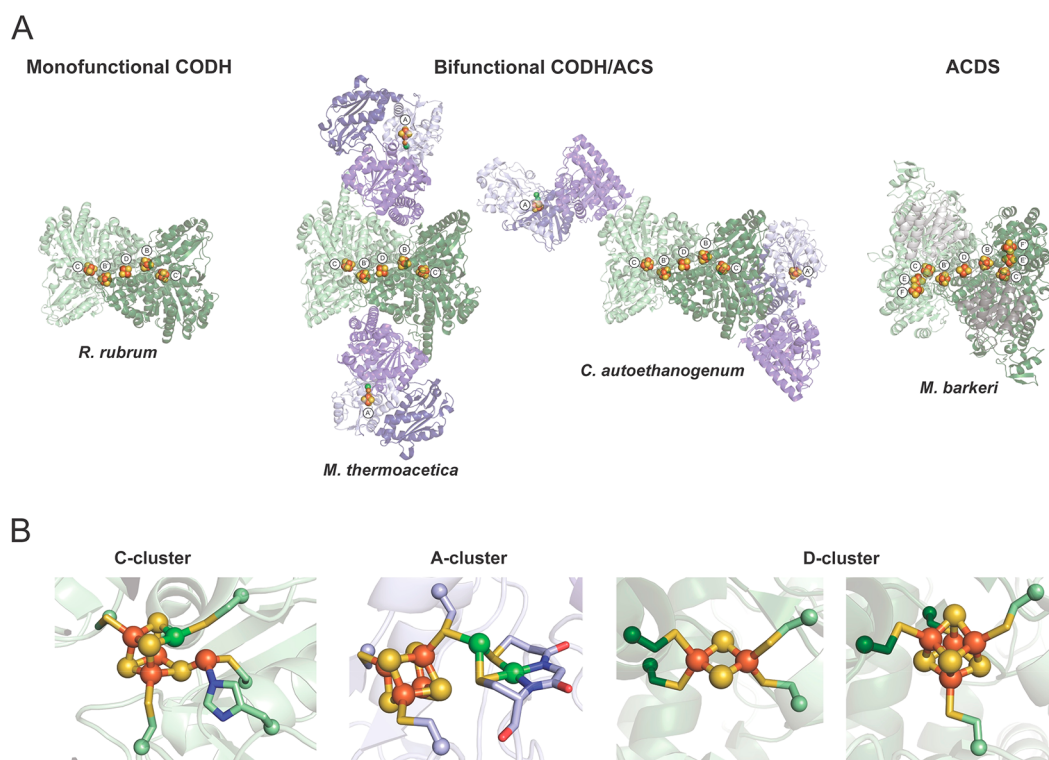
Figure 1. Variations in CODHs. (A) Crystal structures of CODH from *R. rubrum* (PDB entry 1JQK), *M. thermoacetica* (PDB entry 1MJG), *C. autoethanogenum* (PDB entry 6YTT), and *M. barkeri* (PDB entry 3CF4). CODH α_2 is colored light and dark green, and CODH ε_2 is colored light and dark gray. ACS domains 1−3 are colored violet, navy, and light blue, respectively. Metalloclusters are shown as spheres with iron, sulfur, and nickel colored orange, yellow, and green, respectively. *M. barkeri* CODH contains two additional metalloclusters per α monomer, the E- and F-clusters, of unknown function. (B) C-Cluster structure (from *R. rubrum*, PDB entry 1JQK) and A-cluster structure, the latter containing a binuclear metal site bridged by a Cys residue to a [4Fe-4S] cluster (from *M. thermoacetica*, PDB entry 6X5K). Two types of D-clusters are observed in CODH, a unique [2Fe-2S] D-cluster in *Dv*CODH (PDB entry 6B6V) and a more common [4Fe-4S] D-cluster (from *R. rubrum*, PDB entry 1JQK). Nickel ions are colored green, iron ions orange, and sulfur ions yellow. Most side chains shown are truncated at the α carbon.

gain deeper insight into the mechanisms through which CODHs capture and metabolize carbon from the atmosphere and in the microbiome.

CRYSTAL STRUCTURES OF CODHS REVEALED THE SUBUNIT ARCHITECTURE AND THE NATURE OF METALLOCOFACTORS

The first CODH structures were of monofunctional enzymes from *R. rubrum* (*Rr*CODH)[20] and *C. hydrogenoformans* (*Ch*CODH),[21] with structures of CODH from *D. vulgaris* (*Dv*CODH)[22] determined more recently (Table 1). These structures showed that CODH is a homodimer with five metallocofactors: two B-clusters and one D-cluster responsible for wiring electrons to the protein surface from the two Ni−Fe−S-containing catalytic C-clusters buried in the protein (Figure 1A). The C-cluster, which is the site of CO oxidation, contains a [3Fe−4S−Ni] cubane attached via one of the cubane S atoms to a unique Fe site (Figure 1B).[20] Catalysis involves the binding of CO to the Ni ion and the binding of H_2O to the unique Fe (Scheme 3).[23−27]

Electrons generated from CO oxidation travel to the protein surface through the B- and D-clusters, which typically are [4Fe-4S] clusters. However, *Dv*CODH harbors a bridging [2Fe-2S] D-cluster rather than the canonical [4Fe-4S] D-cluster (Figure 1B).[22,28,29] Interestingly, *Dv*CODH is the most oxygen-tolerant of all characterized CODHs.[30] Although *Dv*CODH loses activity upon exposure to oxygen, it is the only known CODH to be fully reactivated upon reduction.[30] To probe the

Scheme 3. Previously Proposed Mechanism of CO Oxidation at the C-Cluster of CODH[23−27 a]
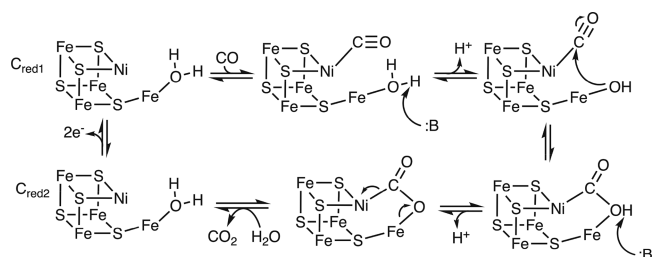
[a]B represents a general base. Cred1 and Cred2 are EPR states that differ by two electrons.

role of the unusual [2Fe-2S] D-cluster in oxygen tolerance, mutagenesis was performed to replace the C−X$_2$−C [2Fe-2S] D-cluster binding motif with the C−X$_7$−C [4Fe-4S] D-cluster motif found in other CODHs. Structural characterization revealed that the [4Fe-4S] D-cluster is partially degraded after 2 h and is lost completely after exposure to oxygen for 2 days, whereas the [2Fe-2S] D-cluster remains intact even after 2 days, suggesting that the [2Fe-2S] D-cluster is a key contributor to the oxygen tolerance of *Dv*CODH.[29]

Following the structural determinations of *Rr*CODH and *Ch*CODH, structures of CODH/ACS from the model acetogen *Moorella thermoacetica* (*Mt*CODH/ACS) were determined.[31,32] These structures showed that the CODH/
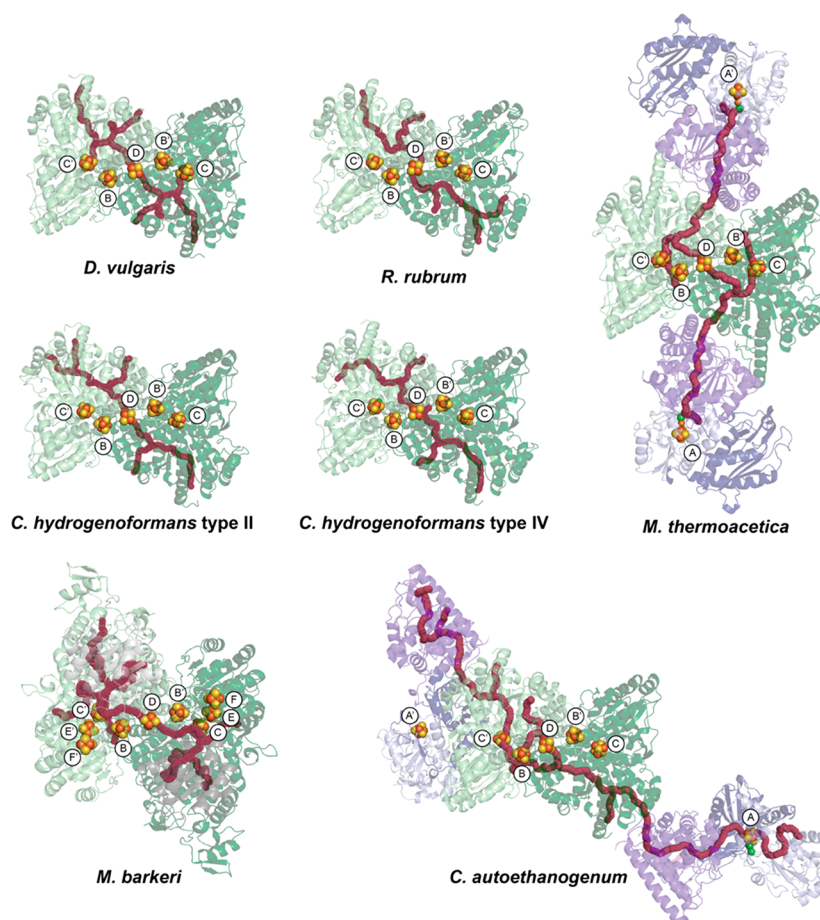
Figure 2. Comparison of gas channels in CODH complexes. All models were superposed on the CODH homodimer and shown with the same orientation. Structures of *D. vulgaris* (PDB entry 6B6V), *R. rubrum* (PDB entry 1JQK), *C. hydrogenoformans* type II (PDB entry 1SU6), *C. hydrogenoformans* type IV (PDB entry 6ELQ), *M. thermoacetica* (PDB entry 1MJG), *M. barkeri* (PDB entry 3CF4), and *C. autoethanogenum* (PDB entry 6YTT). Colored as in Figure 1, with predicted hydrophobic channels colored magenta. Reproduced from ref 38. Copyright 2022 Elsevier.

ACS enzyme complex has one acetyl-CoA synthase protomer bound on either side of a CODH homodimer that was structurally similar to previous CODH structures. More recently, a structure of the bifunctional CODH/ACS from *Clostridium autoethanogenum* (*Ca*CODH/ACS) was determined that demonstrated a mode of binding of ACS to CODH that is substantially different from that of *Mt*CODH/ACS.[33] Although in each case one CODH protomer binds to one ACS protomer, the location of the binding site is distinct. This differential arrangement of subunits creates a CODH/ACS complex that has a different overall shape (Figure 1A). In addition to the B-, C-, and D-clusters, CODH/ACS enzymes have a Ni−Fe−S-containing A-cluster (Figure 1 and Table 1). The A-cluster is the site of acetyl-CoA synthesis and contains a binuclear metal site bridged by a Cys residue to a [4Fe-4S] cluster (Figure 1B).[31] An active A-cluster contains two nickel ions in the binuclear site.[34,35] No structure exists for an intact ACDS complex, but a structure was determined of a heterotetrameric ($\alpha_2\varepsilon_2$) component of *Methanosarcina barkeri* (*Mb*CODH)[23] that contains CODH (Table 1). This CODH structure was similar to previous CODH structures[20,21,36] and revealed the location of two additional metalloclusters: one [4Fe-4S] E-cluster and one [4Fe-4S] F-cluster in each α subunit (Figure 1A).[23]

CRYSTALLOGRAPHIC STUDIES WITH XENON GAS HAVE REVEALED GAS CHANNELS IN CODHS

Structural analyses of CODHs showed that the catalytic C-cluster is buried, requiring a gas channel for CO/CO_2 entry or exit (Figure 1A). In the monofunctional *Dv*CODH and the bifunctional CODH/ACS from *M. thermoacetica* (*Mt*CODH/ACS), the gas channels have been experimentally visualized through xenon crystallographic studies. In these studies, crystals were pressurized with xenon, and when the crystal structure was determined, the xenon sites were used to determine the path of gas channels through the enzymes.[37,38] The *Dv*CODH gas channel originates near the C-cluster and splits into two branches, with one branch leading toward the homodimer interface and the other leading away. Cavity calculations indicate that the gas channels of other monofunctional CODHs, including *Rr*CODH,[18] *Ch*CODH type II,[36] and *Ch*CODH type IV,[39] are likely similar to those of *Dv*CODH (Figure 2).[33]

For the bifunctional CODH/ACS, the gas channels serve the additional purpose of directing the CO generated at the C-cluster to the A-cluster for assembly into acetyl-CoA,[40,41] preventing loss of this valuable metabolic intermediate and potentially protecting other enzymes from CO inhibition. In *Mt*CODH/ACS, the channel leading toward the CODH homodimer interface is conserved and extends further into ACS, leading directly to the A-cluster. The other branch of the
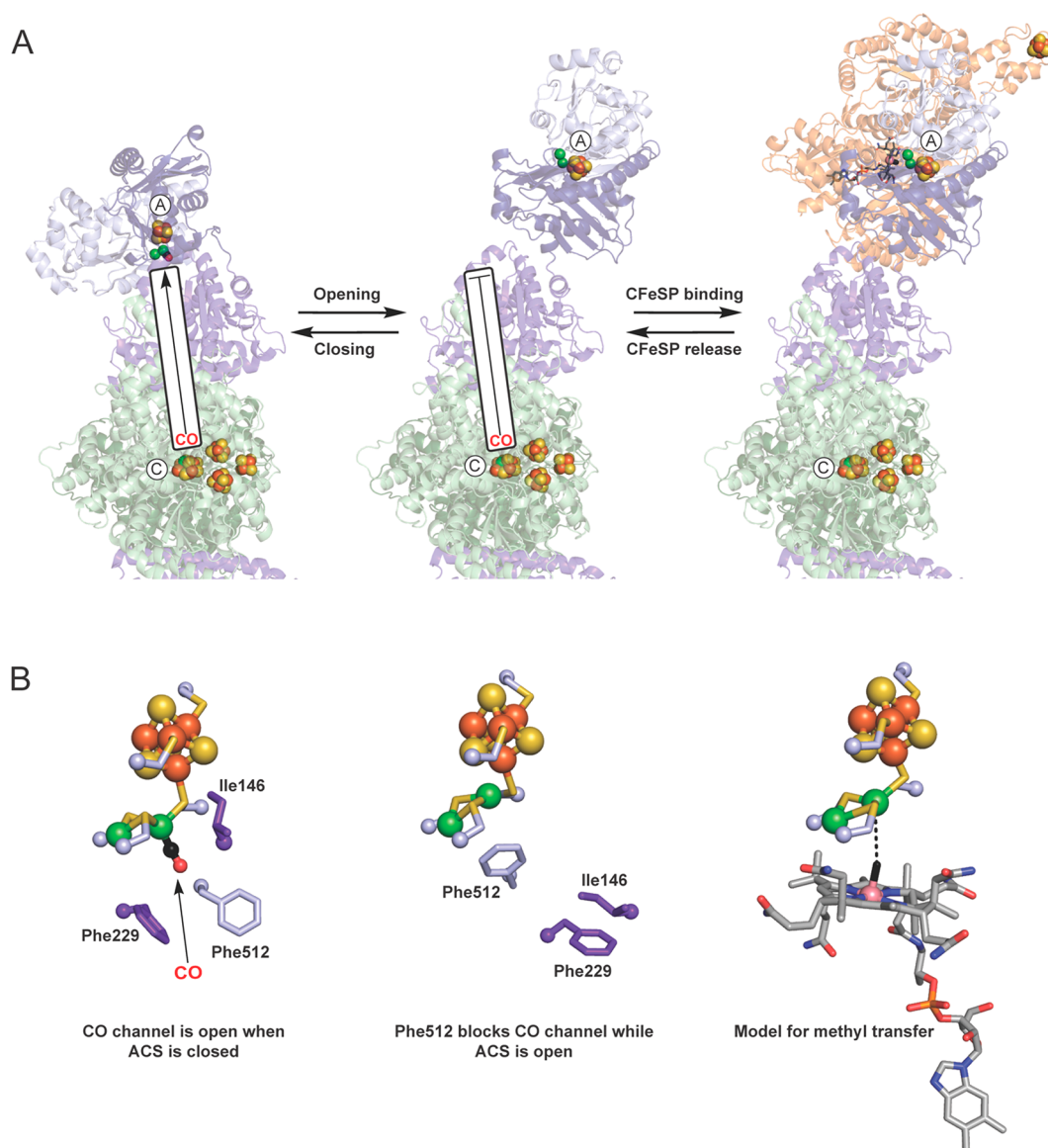
Figure 3. Conformational changes in CODH/ACS facilitate A-cluster carbonylation and methylation. (A) *Mt*CODH/ACS with ACS in the closed, CO-bound conformation (left, PDB entry 6X5K) and in the extended conformation (middle, EMDB entry 21008) and a manual docking of CFeSP (PDB entry 4DJF) to the extended conformation of *Mt*CODH/ACS generated by flexible fitting using negative stain EM data (right). Colored as in Figure 1. CFeSP is colored orange, and the methyl group of methylcobalamin is colored black. (B) CO-bound structure of A-cluster in *Mt*CODH/ACS (left, PDB entry 6X5K), partially open structure of *Mt*CODH/ACS (middle, PDB entry 1OAO), and a close-up of the ACS A-cluster and CFeSP methylcobalamin cofactor from the manual docking model of CFeSP to the extended conformation of CODH/ACS (right). Colored as in panel A.

gas channel observed in *Dv*CODH is absent in *Mt*CODH/ACS; this channel appears to be blocked by bulky aromatic residues.[37,38] In the bifunctional *Ca*CODH/ACS, cavity calculations suggest that the opposite is true, that the channel leading toward the CODH homodimer interface is blocked,[33,38] whereas the channel leading away from the CODH homodimer interface is present. The use of different channels in these two bifunctional CODH/ACS enzymes is likely related to their different quaternary structures. Therefore, the use of alternate gas channels in these different CODH/ACS enzymes would allow CO to be effectively transported along the appropriate path to reach ACS.

In the methanogenic ACDS complex, it is challenging to speculate about the path of the gas channels, as the subunit organization is unknown. In the *Mb*CODH $\alpha_2\varepsilon_2$ structural report,[23] Gong and co-workers suggest that the gas channel in the methanogenic CODH originates from the C-cluster and splits into two branches, with one branch leading to the surface of the protein and the other branch leading to the ε-subunit. This description of the gas channels is relatively consistent with cavity calculations performed on *Mb*CODH, although the calculations suggest additional branching, which may or may not be relevant for gas transport (Figure 2).

■ NEGATIVE STAIN ELECTRON MICROSCOPY HAS PROVIDED VIEWS OF ACS CONFORMATIONAL STATES THAT MUST BE REQUIRED FOR ACETYL-COA SYNTHESIS

The A-cluster of ACS joins together the one-carbon unit from the carbonyl branch of the Wood−Ljungdahl pathway, i.e., the

Scheme 4. Previously Proposed A-Cluster Mechanisms of ACS, Including (A) a Paramagnetic Mechanism of Acetyl-CoA Synthesis at the A-Cluster of ACS[7] and (B) a Diamagnetic Mechanism of Acetyl-CoA Synthesis at the A-Cluster of ACS[53] [a]
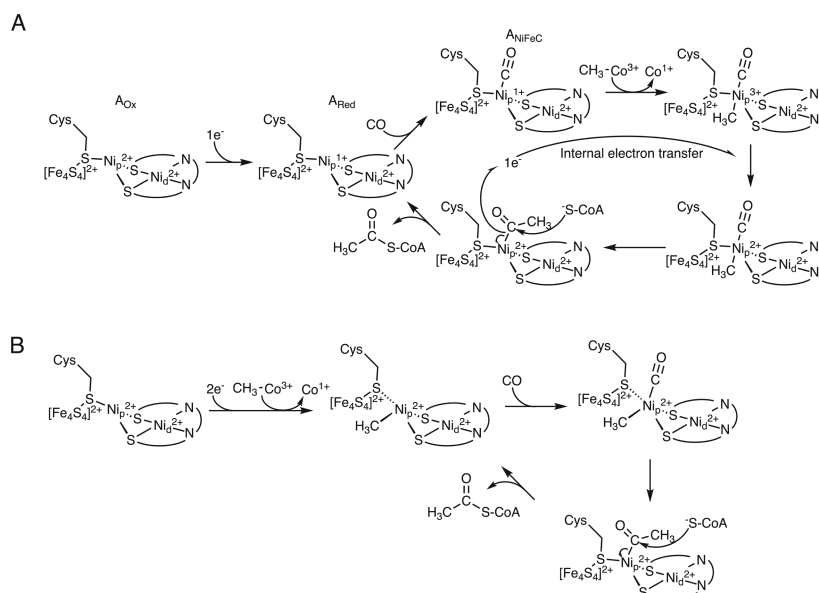
[a] For the sake of simplicity, only one option for binding order is represented in each A-cluster mechanism. Exact oxidation states of metals, in particular Ni_p, are still highly debated and under active investigation.

CO, with the one-carbon unit from the methyl branch, i.e., the methyl group, to generate acetyl-CoA. The CO comes from the C-cluster via the gas channel mentioned above, which is ~70 Å long in MtCODH/ACS (Figure 2).[31,37] The methyl moiety comes from CFeSP and involves an S_N2 transfer of CH_3^+ from a methylcobalamin cofactor to a nickel ion of the A-cluster.[42,43] These two binding events require different conformational states of ACS, a closed-ACS conformation that allows for an open CO channel and an open-ACS conformation that allows for the transfer of a methyl group from CFeSP to the A-cluster (Figure 3A).[37] Although both closed and partially open structures of MtCODH/ACS have been observed crystallographically (Figure 2),[31,32] a conformation of ACS that is sufficiently open to interact with CFeSP for methyl transfer has not been obtained.

Recently, negative stain electron microscopy (EM) has been used to visualize additional conformational states of ACS in the MtCODH/ACS enzyme.[44] These data show that the three-domain ACS subunit can undergo large conformational rearrangements that position two of the three domains into highly extended conformations (Figure 3A).[44] Excitingly, one extended conformation of CODH/ACS seems perfectly oriented to bind CFeSP (Figure 3A).[44,45] Docking of CFeSP to this extended ACS conformation brings the methyl group of methylcobalamin within 4.6 Å of the catalytic nickel of the A-cluster (Figure 3B).[44] Attempts to obtain a structure of a CFeSP in complex with ACS are ongoing.

A RECENT CRYSTAL STRUCTURE PROVIDES A VIEW OF THE CO-BOUND STATE OF THE A-CLUSTER

The CO-bound A-cluster of MtCODH/ACS has been characterized by electron nuclear double resonance,[46] Mössbauer,[47] infrared,[48] and extended X-ray absorption fine structure (EXAFS)[35,49] spectroscopies and has recently been crystallographically observed.[50] The recently reported structure of CO-bound MtCODH/ACS reveals an exclusively tetrahe-

dral geometry for CO bound to the proximal Ni ion (Ni_p).[50] Comparison with previously determined ACS structures indicates that residue Phe512 can rearrange such that the CO channel is open or closed (Figure 3B).[31,32,50,51] Interestingly, this Phe is conserved and the corresponding Phe (Phe195) in the *Methanosarcina thermophila* ACS has been shown to play a role in conformational gating of the A-cluster.[52] However, the exact gating role is likely different in acetogens and methanogens as the domain that contains the CO channel in acetogenic ACS is not found in the methanogenic enzyme. In MtCODH/ACS, when its CO channel is open and CO is bound to the A-cluster, a different Phe, Phe229, packs against the CO ligand, potentially helping to stabilize the CO-bound state (Figure 3B).[50] Additionally, Ile146 packs against Ni_p, enforcing the tetrahedral geometry of the CO−Ni_p and preventing the binding of a second CO, which would be expected to inhibit the A-cluster (Figure 3B).[50] In the more open conformation of CODH/ACS, Ile146 is displaced from Ni_p,[32] creating space for Ni_p to adopt a square planar geometry, which is proposed to be required for A-cluster methylation.[32]

THE MECHANISM OF THE A-CLUSTER IS STILL CONTROVERSIAL

Two mechanisms for the A-cluster have been proposed: the paramagnetic and diamagnetic mechanisms (Scheme 4).[7,53] In the paramagnetic mechanism, the as-isolated state, Ni_p^{2+}, is named A_{Ox}. A_{Ox} undergoes reductive activation to give A_{Red}, with Ni_p^+. Ni_p^+ may then be carbonylated to generate a Ni_p^+−CO species, named A_{NiFeC} due to ^{61}Ni, ^{13}C, and ^{57}Fe hyperfine interactions exhibited in its electron paramagnetic resonance (EPR) spectrum.[46,54] Upon methylation, a Ni_p^{3+}−CH_3 species is proposed to form. However, EPR spectroscopy of methylated ACS indicates a diamagnetic product,[55,56] rather than a paramagnetic Ni_p^{3+}−CH_3 species, so the previously proposed paramagnetic mechanism includes an internal electron transfer to form Ni_p^{2+}−CH_3. In the final step of the

paramagnetic mechanism, the acetylated A-cluster undergoes nucleophilic acyl substitution with nucleophilic attack by CoA, thereby giving the acetyl-CoA product and regenerating A_{Red}. Along with characterization of the A_{NiFeC} state, nickel-substituted azurin models of ACS have been shown to generate Ni^+-CO and $Ni^{3+}-CH_3$ species, which is consistent with a paramagnetic mechanism.[57−59]

In the diamagnetic mechanism, Ni_p^0 is proposed to be carbonylated to give Ni_p^0-CO and methylated to give $Ni_p^{2+}-CH_3$.[53] The formation of the $Ni_p^{2+}-CH_3$ intermediate is consistent with the observation that the methylated state of the A-cluster is EPR silent.[55,56] There is ACS model chemistry that supports a diamagnetic mechanism in which zerovalent nickel complexes can be successfully methylated to generate $Ni^{2+}-CH_3$ species.[60,61] However, a Ni_p^0 species has never been reported in ACS. Another unresolved question regarding the mechanism of ACS catalysis is the order of substrate binding, i.e., whether methylation occurs prior to carbonylation[60−62] or whether substrate binding occurs through a random sequential mechanism.[63]

CONCLUSIONS AND FUTURE WORK

Although there have been significant advances in our understanding of CODH and its partners in one-carbon metabolism, there is still much to learn. Resolving the controversy around the mechanism of the A-cluster is just one example. Structural biology will likely continue to provide important insights. Although CODH/ACS has been structurally characterized, the complex between ACS and CFeSP has not been experimentally visualized. This structure could provide important insight into the mechanism of the A-cluster, addressing, for example, whether a carbonylated A-cluster is structurally compatible with methylation or if the S_N2 reaction requires a Ni_p that has no other ligand bound. Additionally, the ACDS complex has not been structurally characterized. Visualizing the ACDS complex would undoubtedly allow for a deeper understanding of the mechanism of acetyl-CoA cleavage. Notably, CFeSP is a fascinating enzyme in its own right. In addition to methylating ACS, acetogenic CFeSP must employ the corrinoid as a supernucleophile to remove a methyl group from methyltetrahydrofolate in a reaction that involves dramatic protein conformational changes.[45] CFeSP must also be activated before it can perform this task, and work by the Dobbek group has begun to unravel how this activation progress occurs.[64,65]

The connection between human health and the relative abundance of CODH-containing microbes in the gut microbiota is actively being investigated. Interestingly, a recent study has identified the Wood−Ljungdahl pathway as a route for disposing of reducing equivalents in the intestinal pathogen *Clostridium difficile*, suggesting a largely unexplored role for CODH in *C. difficile* pathogenesis.[66] Through further study of CODH and its partners in anaerobic one-carbon metabolism, we will deepen our understanding of the roles that CODHs play in carbon flux, both within our microbiome and more broadly in our atmosphere.

AUTHOR INFORMATION

Corresponding Author

Catherine L. Drennan − *Department of Chemistry, Massachusetts Institute of Technology, Cambridge, Massachusetts 02139, United States; Department of Biology, Massachusetts Institute of Technology, Cambridge, Massachusetts 02139, United States; Howard Hughes Medical Institute, Massachusetts Institute of Technology, Cambridge, Massachusetts 02139, United States; Bio-inspired Solar Energy Program, Canadian Institute for Advanced Research, Toronto, ON M5G 1M1, Canada;* ● orcid.org/0000-0001-5486-2755; Email: cdrennan@mit.edu

Authors

Alison Biester − *Department of Chemistry, Massachusetts Institute of Technology, Cambridge, Massachusetts 02139, United States;* ● orcid.org/0000-0003-4129-1871

Andrea N. Marcano-Delgado − *Department of Chemistry, Massachusetts Institute of Technology, Cambridge, Massachusetts 02139, United States*

Complete contact information is available at:
https://pubs.acs.org/10.1021/acs.biochem.2c00425

Notes

The authors declare no competing financial interest.

ABBREVIATIONS

CODH, carbon monoxide dehydrogenase; ACS, acetyl-CoA synthase; CFeSP, corrinoid iron−sulfur protein; ACDS, acetyl-CoA decarbonylase/synthase.

REFERENCES

(1) Adam, P. S.; Borrel, G.; Gribaldo, S. Evolutionary history of carbon monoxide dehydrogenase/acetyl-CoA synthase, one of the oldest enzymatic complexes. *Proc. Natl. Acad. Sci. U. S. A.* **2018**, *115* (6), No. E1166-E1173.

(2) Gaci, N.; Borrel, G.; Tottey, W.; O'Toole, P. W.; Brugère, J.-F. Archaea and the human gut: new beginning of an old story. *World J. Gastroenterol.* **2014**, *20* (43), 16062−16078.

(3) Li, Z.; Wang, X.; Alberdi, A.; Deng, J.; Zhong, Z.; Si, H.; Zheng, C.; Zhou, H.; Wang, J.; Yang, Y.; Wright, A.-D. G.; Mao, S.; Zhang, Z.; Guan, L.; Li, G. Comparative microbiome analysis reveals the ecological relationships between rumen methanogens, acetogens, and their hosts. *Front. Microbiol.* **2020**, *11*, 1311.

(4) Matson, E. G.; Gora, K. G.; Leadbetter, J. R. Anaerobic carbon monoxide dehydrogenase diversity in the homoacetogenic hindgut microbial communities of lower termites and the wood roach. *PLoS One* **2011**, *6* (4), No. e19316.

(5) Appel, A. M.; Bercaw, J. E.; Bocarsly, A. B.; Dobbek, H.; DuBois, D. L.; Dupuis, M.; Ferry, J. G.; Fujita, E.; Hille, R.; Kenis, P. J. A.; Kerfeld, C. A.; Morris, R. H.; Peden, C. H. F.; Portis, A. R.; Ragsdale, S. W.; Rauchfuss, T. B.; Reek, J. N. H.; Seefeldt, L. C.; Thauer, R. K.; Waldrop, G. L. Frontiers, opportunities, and challenges in biochemical and chemical catalysis of CO_2 fixation. *Chem. Rev.* **2013**, *113* (8), 6621−6658.

(6) Can, M.; Armstrong, F. A.; Ragsdale, S. W. Structure, function, and mechanism of the nickel metalloenzymes, CO dehydrogenase, and acetyl-CoA synthase. *Chem. Rev.* **2014**, *114* (8), 4149−74.

(7) Ragsdale, S. W. Life with carbon monoxide. *Crit. Rev. Biochem. Mol. Biol.* **2004**, *39* (3), 165−195.

(8) Kung, Y.; Drennan, C. L. One-carbon chemistry of nickel-containing carbon monoxide dehydrogenase and acetyl-CoA synthase. In *The Biological Chemistry of Nickel*; Zamble, D., Rowińska-Żyrek, M., Kozlowski, H., Eds.; The Royal Society of Chemistry, 2017; pp 121−148.

(9) Bartholomew, G. W.; Alexander, M. Microbial metabolism of carbon monoxide in culture and in soil. *Appl. Environ. Microbiol.* **1979**, *37* (5), 932−937.

(10) Byrne, J. D.; Gallo, D.; Boyce, H.; Becker, S. L.; Kezar, K. M.; Cotoia, A. T.; Feig, V. R.; Lopes, A.; Csizmadia, E.; Longhi, M. S.; Lee, J. S.; Kim, H.; Wentworth, A. J.; Shankar, S.; Lee, G. R.; Bi, J.; Witt, E.; Ishida, K.; Hayward, A.; Kuosmanen, J. L. P.; Jenkins, J.; Wainer, J.; Aragon, A.; Wong, K.; Steiger, C.; Jeck, W. R.; Bosch, D. E.; Coleman, M. C.; Spitz, D. R.; Tift, M.; Langer, R.; Otterbein, L. E.; Traverso, G. Delivery of therapeutic carbon monoxide by gas-entrapping materials. *Sci. Transl. Med.* **2022**, *14* (651), No. eabl4135.

(11) Hopper, C. P.; De La Cruz, L. K.; Lyles, K. V.; Wareham, L. K.; Gilbert, J. A.; Eichenbaum, Z.; Magierowski, M.; Poole, R. K.; Wollborn, J.; Wang, B. Role of carbon monoxide in host-gut microbiome communication. *Chem. Rev.* **2020**, *120* (24), 13273−13311.

(12) Ragsdale, S. W.; Pierce, E. Acetogenesis and the Wood-Ljungdahl pathway of CO_2 fixation. *Biochim. Biophys. Acta - Proteins Proteom.* **2008**, *1784* (12), 1873−1898.

(13) Drake, H. L. Acetogenesis, acetogenic bacteria, and the acetyl-CoA "Wood/Ljungdahl" pathway: past and current perspectives. In *Acetogenesis*; Drake, H. L., Ed.; Springer US: Boston, 1994; pp 3−60.

(14) Lajoie, S. F.; Bank, S.; Miller, T. L.; Wolin, M. J. Acetate production from hydrogen and [^{13}C]carbon dioxide by the microflora of human feces. *Appl. Environ. Microbiol.* **1988**, *54* (11), 2723−2727.

(15) Wolin, M. J.; Miller, T. L. Acetogenesis from CO_2 in the human colonic ecosystem. In *Acetogenesis*; Springer, 1994; pp 365−385.

(16) Thauer, R. K.; Kaster, A. K.; Seedorf, H.; Buckel, W.; Hedderich, R. Methanogenic archaea: ecologically relevant differences in energy conservation. *Nat. Rev. Microbiol.* **2008**, *6* (8), 579−91.

(17) Thauer, R. K. Biochemistry of methanogenesis: a tribute to Marjory Stephenson: 1998 Marjory Stephenson prize lecture. *Microbiology* **1998**, *144* (9), 2377−2406.

(18) Kocsis, E.; Kessel, M.; DeMoll, E.; Grahame, D. A. Structure of the Ni/Fe-S protein subcomponent of the acetyl-CoA decarbonylase/synthase complex from *Methanosarcina thermophila* at 26-Å resolution. *J. Struct. Biol.* **1999**, *128* (2), 165−174.

(19) Grahame, D. A. Catalysis of acetyl-CoA cleavage and tetrahydrosarcinapterin methylation by a carbon monoxide dehydro-genase-corrinoid enzyme complex. *J. Biol. Chem.* **1991**, *266* (33), 22227−22233.

(20) Drennan, C. L.; Heo, J.; Sintchak, M. D.; Schreiter, E.; Ludden, P. W. Life on carbon monoxide: X-ray structure of *Rhodospirillum rubrum* Ni-Fe-S carbon monoxide dehydrogenase. *Proc. Natl. Acad. Sci. U.S.A.* **2001**, *98* (21), 11973−11978.

(21) Dobbek, H.; Svetlitchnyi, V.; Gremer, L.; Huber, R.; Meyer, O. Crystal structure of a carbon monoxide dehydrogenase reveals a [Ni-4Fe-5S] cluster. *Science* **2001**, *293* (5533), 1281−1285.

(22) Wittenborn, E. C.; Merrouch, M.; Ueda, C.; Fradale, L.; Léger, C.; Fourmond, V.; Pandelia, M.-E.; Dementin, S.; Drennan, C. L. Redox-dependent rearrangements of the NiFeS cluster of carbon monoxide dehydrogenase. *eLife* **2018**, *7*, No. e39451.

(23) Gong, W.; Hao, B.; Wei, Z.; Ferguson, D. J., Jr.; Tallant, T.; Krzycki, J. A.; Chan, M. K. Structure of the $\alpha_2\varepsilon_2$ Ni-dependent CO dehydrogenase component of the *Methanosarcina barkeri* acetyl-CoA decarbonylase/synthase complex. *Proc. Natl. Acad. Sci. U.S.A.* **2008**, *105* (28), 9558−9563.

(24) Kung, Y.; Doukov, T. I.; Seravalli, J.; Ragsdale, S. W.; Drennan, C. L. Crystallographic snapshots of cyanide- and water-bound C-clusters from bifunctional carbon monoxide dehydrogenase/acetyl-CoA synthase. *Biochemistry* **2009**, *48* (31), 7432−7440.

(25) Jeoung, J. H.; Dobbek, H. Carbon dioxide activation at the Ni,Fe-cluster of anaerobic carbon monoxide dehydrogenase. *Science* **2007**, *318* (5855), 1461−4.

(26) Kung, Y.; Drennan, C. L. A role for nickel-iron cofactors in biological carbon monoxide and carbon dioxide utilization. *Curr. Opin. Chem. Biol.* **2011**, *15* (2), 276−283.

(27) Jeoung, J.-H.; Dobbek, H. Structural basis of cyanide inhibition of Ni, Fe-containing carbon monoxide dehydrogenase. *J. Am. Chem. Soc.* **2009**, *131* (29), 9922−9923.

(28) Wittenborn, E. C.; Cohen, S. E.; Merrouch, M.; Léger, C.; Fourmond, V.; Dementin, S.; Drennan, C. L. Structural insight into metallocofactor maturation in carbon monoxide dehydrogenase. *J. Biol. Chem.* **2019**, *294* (35), 13017−13026.

(29) Wittenborn, E. C.; Guendon, C.; Merrouch, M.; Benvenuti, M.; Fourmond, V.; Léger, C.; Drennan, C. L.; Dementin, S. The solvent-exposed Fe-S D-cluster contributes to oxygen-resistance in *Desulfovibrio vulgaris* Ni-Fe carbon monoxide dehydrogenase. *ACS Catal.* **2020**, *10* (13), 7328−7335.

(30) Merrouch, M.; Hadj-Saïd, J.; Domnik, L.; Dobbek, H.; Léger, C.; Dementin, S.; Fourmond, V. O_2 inhibition of Ni-containing CO dehydrogenase is partly reversible. *Chem. - Eur. J.* **2015**, *21* (52), 18934−18938.

(31) Doukov, T. I.; Iverson, T. M.; Seravalli, J.; Ragsdale, S. W.; Drennan, C. L. A Ni-Fe-Cu center in a bifunctional carbon monoxide dehydrogenase/acetyl-CoA synthase. *Science* **2002**, *298* (5593), 567−572.

(32) Darnault, C.; Volbeda, A.; Kim, E. J.; Legrand, P.; Vernède, X.; Lindahl, P. A.; Fontecilla-Camps, J. C. Ni-Zn-[Fe_4-S_4] and Ni-Ni-[Fe_4-S_4] clusters in closed and open α subunits of acetyl-CoA synthase/carbon monoxide dehydrogenase. *Nat. Struct. Mol. Biol.* **2003**, *10* (4), 271−279.

(33) Lemaire, O. N.; Wagner, T. Gas channel rerouting in a primordial enzyme: Structural insights of the carbon-monoxide dehydrogenase/acetyl-CoA synthase complex from the acetogen *Clostridium autoethanogenum*. *Biochim. Biophys. Acta - Bioenerg* **2021**, *1862* (1), 148330−148330.

(34) Bramlett, M. R.; Tan, X.; Lindahl, P. A. Inactivation of acetyl-CoA synthase/carbon monoxide dehydrogenase by copper. *J. Am. Chem. Soc.* **2003**, *125* (31), 9316−9317.

(35) Seravalli, J.; Xiao, Y.; Gu, W.; Cramer, S. P.; Antholine, W. E.; Krymov, V.; Gerfen, G. J.; Ragsdale, S. W. Evidence that NiNi acetyl-CoA synthase is active and that the CuNi enzyme is not. *Biochemistry* **2004**, *43* (13), 3944−3955.

(36) Dobbek, H.; Svetlitchnyi, V.; Liss, J.; Meyer, O. Carbon monoxide induced decomposition of the active site [Ni-4Fe-5S] cluster of CO dehydrogenase. *J. Am. Chem. Soc.* **2004**, *126* (17), 5382−5387.

(37) Doukov, T. I.; Blasiak, L. C.; Seravalli, J.; Ragsdale, S. W.; Drennan, C. L. Xenon in and at the end of the tunnel of bifunctional carbon monoxide dehydrogenase/acetyl-CoA synthase. *Biochemistry* **2008**, *47* (11), 3474−3483.

(38) Biester, A.; Dementin, S.; Drennan, C. L. Visualizing the gas channel of a monofunctional carbon monoxide dehydrogenase. *J. Inorg. Biochem.* **2022**, *230*, 111774.

(39) Domnik, L.; Merrouch, M.; Goetzl, S.; Jeoung, J. H.; Léger, C.; Dementin, S.; Fourmond, V.; Dobbek, H. CODH-IV: a high-efficiency CO-scavenging CO dehydrogenase with resistance to O_2. *Angew. Chem., Int. Ed.* **2017**, *56* (48), 15466−15469.

(40) Seravalli, J.; Ragsdale, S. W. Channeling of carbon monoxide during anaerobic carbon dioxide fixation. *Biochemistry* **2000**, *39* (6), 1274−1277.

(41) Tan, X.; Loke, H.-K.; Fitch, S.; Lindahl, P. A. The tunnel of acetyl-coenzyme a synthase/carbon monoxide dehydrogenase regulates delivery of CO to the active site. *J. Am. Chem. Soc.* **2005**, *127* (16), 5833−5839.

(42) Menon, S.; Ragsdale, S. W. Role of the [4Fe-4S] cluster in reductive activation of the cobalt center of the corrinoid iron-sulfur protein from *Clostridium thermoaceticum* during acetate biosynthesis. *Biochemistry* **1998**, *37* (16), 5689−5698.

(43) Menon, S.; Ragsdale, S. W. The role of an iron-sulfur cluster in an enzymatic methylation reaction: methylation of CO dehydrogen-

ase/acetyl-CoA synthase by the methylated corrinoid iron-sulfur protein. *J. Biol. Chem.* **1999**, *274* (17), 11513−11518.

(44) Cohen, S. E.; Brignole, E. J.; Wittenborn, E. C.; Can, M.; Thompson, S.; Ragsdale, S. W.; Drennan, C. L. Negative-stain electron microscopy reveals dramatic structural rearrangements in Ni-Fe-S-dependent carbon monoxide dehydrogenase/acetyl-CoA synthase. *Structure* **2021**, *29*, 43−49.e3.

(45) Kung, Y.; Ando, N.; Doukov, T. I.; Blasiak, L. C.; Bender, G.; Seravalli, J.; Ragsdale, S. W.; Drennan, C. L. Visualizing molecular juggling within a B₁₂-dependent methyltransferase complex. *Nature* **2012**, *484* (7393), 265−269.

(46) Fan, C. L.; Gorst, C. M.; Ragsdale, S. W.; Hoffman, B. M. Characterization of the Ni-Fe-C complex formed by reaction of carbon monoxide with the carbon monoxide dehydrogenase from *Clostridium thermoaceticum* by Q-band ENDOR. *Biochemistry* **1991**, *30* (2), 431−435.

(47) Lindahl, P. A.; Ragsdale, S. W.; Münck, E. Mössbauer study of CO dehydrogenase from *Clostridium thermoaceticum*. *J. Biol. Chem.* **1990**, *265* (7), 3880−3888.

(48) Kumar, M.; Ragsdale, S. W. Characterization of the carbon monoxide binding site of carbon monoxide dehydrogenase from *Clostridium thermoaceticum* by infrared spectroscopy. *J. Am. Chem. Soc.* **1992**, *114* (22), 8713−8715.

(49) Can, M.; Giles, L. J.; Ragsdale, S. W.; Sarangi, R. X-ray absorption spectroscopy reveals an organometallic Ni-C bond in the CO-treated form of acetyl-CoA synthase. *Biochemistry* **2017**, *56* (9), 1248−1260.

(50) Cohen, S. E.; Can, M.; Wittenborn, E. C.; Hendrickson, R. A.; Ragsdale, S. W.; Drennan, C. L. Crystallographic characterization of the carbonylated A-cluster in carbon monoxide dehydrogenase/acetyl-CoA synthase. *ACS Catal.* **2020**, *10* (17), 9741−9746.

(51) Svetlitchnyi, V.; Dobbek, H.; Meyer-Klaucke, W.; Meins, T.; Thiele, B.; Römer, P.; Huber, R.; Meyer, O. A functional Ni-Ni-[4Fe-4S] cluster in the monomeric acetyl-CoA synthase from *Carboxydothermus hydrogenoformans*. *Proc. Natl. Acad. Sci. U.S.A.* **2004**, *101* (2), 446−451.

(52) Gencic, S.; Kelly, K.; Ghebreamlak, S.; Duin, E. C.; Grahame, D. A. Different modes of carbon monoxide binding to acetyl-CoA synthase and the role of a conserved phenylalanine in the coordination environment of nickel. *Biochemistry* **2013**, *52* (10), 1705−1716.

(53) Lindahl, P. A. Acetyl-coenzyme A synthase: the case for a Ni_p^0-based mechanism of catalysis. *J. Biol. Inorg. Chem.* **2004**, *9* (5), 516−524.

(54) Ragsdale, S. W.; Wood, H. G.; Antholine, W. E. Evidence that an iron-nickel-carbon complex is formed by reaction of CO with the CO dehydrogenase from *Clostridium thermoaceticum*. *Proc. Natl. Acad. Sci. U.S.A.* **1985**, *82* (20), 6811−6814.

(55) Barondeau, D. P.; Lindahl, P. A. Methylation of carbon monoxide dehydrogenase from *Clostridium thermoaceticum* and mechanism of acetyl coenzyme A synthesis. *J. Am. Chem. Soc.* **1997**, *119* (17), 3959−3970.

(56) Seravalli, J.; Kumar, M.; Ragsdale, S. W. Rapid kinetic studies of acetyl-CoA synthesis: evidence supporting the catalytic intermediacy of a paramagnetic NiFeC species in the autotrophic Wood-Ljungdahl pathway. *Biochemistry* **2002**, *41* (6), 1807−1819.

(57) Manesis, A. C.; Musselman, B. W.; Keegan, B. C.; Shearer, J.; Lehnert, N.; Shafaat, H. S. A biochemical nickel(I) state supports nucleophilic alkyl addition: a roadmap for methyl reactivity in acetyl coenzyme A synthase. *Inorg. Chem.* **2019**, *58* (14), 8969−8982.

(58) Manesis, A. C.; O'Connor, M. J.; Schneider, C. R.; Shafaat, H. S. Multielectron chemistry within a model nickel metalloprotein: mechanistic implications for acetyl-CoA synthase. *J. Am. Chem. Soc.* **2017**, *139* (30), 10328−10338.

(59) Manesis, A. C.; Shafaat, H. S. Electrochemical, spectroscopic, and density functional theory characterization of redox activity in nickel-substituted azurin: a model for acetyl-CoA synthase. *Inorg. Chem.* **2015**, *54* (16), 7959−7967.

(60) Eckert, N. A.; Dougherty, W. G.; Yap, G. P. A.; Riordan, C. G. Methyl transfer from methylcobaloxime to (triphos)Ni(PPh₃): relevance to the mechanism of acetyl coenzyme A synthase. *J. Am. Chem. Soc.* **2007**, *129* (30), 9286−9287.

(61) Ito, M.; Kotera, M.; Matsumoto, T.; Tatsumi, K. Dinuclear nickel complexes modeling the structure and function of the acetyl CoA synthase active site. *Proc. Natl. Acad. Sci. U.S.A.* **2009**, *106* (29), 11862−11866.

(62) Gencic, S.; Duin, E. C.; Grahame, D. A. Tight coupling of partial reactions in the acetyl-CoA decarbonylase/synthase (ACDS) multienzyme complex from *Methanosarcina thermophila*: acetyl C-C bond fragmentation at the A-cluster promoted by protein conformational changes. *J. Biol. Chem.* **2010**, *285* (20), 15450−15463.

(63) Seravalli, J.; Ragsdale, S. W. Pulse-chase studies of the synthesis of acetyl-CoA by carbon monoxide dehydrogenase/acetyl-CoA synthase: evidence for a random mechanism of methyl and carbonyl addition. *J. Biol. Chem.* **2008**, *283* (13), 8384−94.

(64) Hennig, S. E.; Goetzl, S.; Jeoung, J.-H.; Bommer, M.; Lendzian, F.; Hildebrandt, P.; Dobbek, H. ATP-induced electron transfer by redox-selective partner recognition. *Nat. Commun.* **2014**, *5*, 4626.

(65) Goetzl, S.; Teutloff, C.; Werther, T.; Hennig, S. E.; Jeoung, J.-H.; Bittl, R.; Dobbek, H. Protein dynamics in the reductive activation of a B12-containing enzyme. *Biochemistry* **2017**, *56* (41), 5496−5502.

(66) Gencic, S.; Grahame, D. A.; Metcalf, W. W. Diverse energy-conserving pathways in *Clostridium difficile*: growth in the absence of amino acid stickland acceptors and the role of the Wood-Ljungdahl pathway. *J. Bacteriol.* **2020**, *202* (20), No. e00233-20.